Cellular Signalling 58 (2019) 79–90

Contents lists available at ScienceDirect

Cellular Signalling

journal homepage: www.elsevier.com/locate/cellsig

Comparative transcriptomics reveals mechanisms underlying *cln3*-deficiency phenotypes in *Dictyostelium*

Robert J. Huber*, Sabateeshan Mathavarajah

Department of Biology, Trent University, Peterborough, Ontario, Canada

ARTICLE INFO

Keywords:
Batten disease
Neuronal ceroid lipofuscinosis
CLN3
Dictyostelium discoideum
RNA sequencing

ABSTRACT

Mutations in *CLN3* cause a juvenile form of neuronal ceroid lipofuscinosis (NCL). This devastating neurological disorder, commonly known as Batten disease, is currently untreatable due to a lack of understanding of the physiological role of the protein. Recently, work in the social amoeba *Dictyostelium discoideum* has provided valuable new insight into the function of CLN3 in the cell. More specifically, research has linked the *Dictyostelium* homolog (gene: *cln3*, protein: Cln3) to protein secretion, adhesion, and aggregation during starvation, which initiates multicellular development. In this study, we used comparative transcriptomics to explore the mechanisms underlying the aberrant response of *cln3*$^-$ cells to starvation. During starvation, 1153 genes were differentially expressed in *cln3*$^-$ cells compared to WT. Among the differentially expressed genes were homologs of other human NCL genes including *TPP1/CLN2*, *CLN5*, *CTSD/CLN10*, *PGRN/CLN11*, and *CTSF/CLN13*. STRING and GO term analyses revealed an enrichment of genes linked to metabolic, biosynthetic, and catalytic processes. We then coupled the findings from the RNA-seq analysis to biochemical assays, specifically showing that loss of *cln3* affects the expression and activity of lysosomal enzymes, increases endo-lysosomal pH, and alters nitric oxide homeostasis. Finally, we show that *cln3*$^-$ cells accumulate autofluorescent storage bodies during starvation and provide evidence linking the function of Cln3 to Tpp1 and CtsD activity. In total, this study enhances our knowledge of the molecular mechanisms underlying Cln3 function in *Dictyostelium*.

1. Introduction

The neuronal ceroid lipofuscinoses (NCLs) are forms of neurodegeneration that can affect people of all ages and ethnicities [1]. Also known as Batten disease, this devastating and incurable neurological disorder is the most common form of childhood neurodegeneration [1]. The hallmark of the disease is the accumulation of autofluorescent storage bodies in almost every cell type and organ [2,3]. Storage body accumulation is a result of lysosomal dysfunction, that gradually leads to vision loss, seizures, impaired cognitive and motor function, and premature death [4]. Unfortunately, the mechanisms underlying Batten disease are not well understood and the physiological functions of the proteins associated with the disease have not been fully established.

The most common subtype of Batten disease is caused by loss-of-function mutations in ceroid lipofuscinosis neuronal 3 (*CLN3*) [1,4]. The CLN3 protein is conserved from yeast to human and is speculated to play a role in apoptosis, autophagy, adhesion, cell cycle control, endocytosis, multicellular development, osmoregulation, pH and ion homeostasis, and protein secretion and trafficking [5–13]. However, the precise function of CLN3 has yet to be revealed.

Recent work using the model system *Dictyostelium discoideum* has provided fresh new insight into the possible function of CLN3 in mammalian cells. *Dictyostelium* has a unique life cycle that allows for the effects of gene deficiency to be studied at both the single cell and multicellular level [14]. This model organism is also recognized as an excellent system for studying the functions of proteins underlying neurological disorders, including the NCLs [15,16]. When exposed to nutrients, *Dictyostelium* amoeba grow and divide by mitosis. When starved, cells halt growth and enter a multicellular developmental program that concludes with the formation of a fruiting body after 24 h. In *Dictyostelium*, loss of the CLN3 homolog (gene: *cln3*, protein: Cln3) reduces adhesion, de-regulates protein secretion, alters osmoregulation,

Abbreviations: AprA, autocrine proliferation repressor; CfaD, counting factor-associated protein; CLN, ceroid lipofuscinosis neuronal; CmfA, conditioned media factor; COG, conserved oligomeric Golgi; CtnA, countin; CTS, cathepsin; FDR, false discovery rate; GluA, beta-glucosidase; GRN, granulin; LAGO, A logically accelerated GO term finder; NCL, neuronal ceroid lipofuscinosis; NagA, *N*-acetylglucosaminidase; NO, nitric oxide; PGRN, progranulin; TGN, trans-Golgi network; TPP1, tripeptidyl peptidase; Vat, V-ATPase subunit; Vmp1, vacuole membrane protein

* Corresponding author at: Trent University, Department of Biology, 1600 West Bank Drive, Peterborough, Ontario K9L 0G2, Canada.
E-mail address: roberthuber@trentu.ca (R.J. Huber).

https://doi.org/10.1016/j.cellsig.2019.02.004
Received 25 November 2018; Received in revised form 29 January 2019; Accepted 9 February 2019
Available online 14 February 2019
0898-6568/ © 2019 Elsevier Inc. All rights reserved.

and causes cells to develop precociously [7–9,11]. However, the molecular mechanisms underlying these phenotypes are not yet known.

A recent study in *Dictyostelium* used RNA-seq coupled with cellular and biochemical assays to reveal an osmoregulatory defect in *cln3*$^-$ cells [11]. The gene expression analysis not only provided insight into the genes differentially expressed during osmotic stress, but it also revealed that *cln3*-deficiency increases the expression and activity of the *Dictyostelium* homolog of human tripeptidyl peptidase 1 (TPP1, causes CLN2 disease in humans) [11]. In addition to an osmoregulatory defect, previous work also revealed that loss of *cln3* impairs protein secretion, reduces adhesion, and delays aggregation during the first 6 h of multicellular development [7–9]. However, those previous studies did not use RNA-seq to explore the transcriptional changes underlying these phenotypes. Therefore, in this study, we performed a new RNA-seq analysis to gain insight into the molecular mechanisms underlying *cln3*-deficiency phenotypes during the early stages of multicellular development. Following an analysis of the differentially expressed genes, we performed cellular and biochemical assays to validate the observed differences in gene expression between WT and *cln3*$^-$ cells. In total, this study explores the molecular mechanisms underlying the response of *cln3*$^-$ cells to starvation, as well as reveals previously undescribed phenotypes, which ultimately provides new insight into the physiological role of Cln3 in the cell.

2. Materials and methods

2.1. Cell lines, media, chemicals, antibodies, and statistical analysis

Cells were maintained on SM agar with *Klebsiella aerogenes*. Cells were also cultured axenically in HL5 medium at room temperature and 150 rpm. Cultures were supplemented with ampicillin (100 μg/ml) and streptomycin sulfate (300 μg/ml) to prevent bacterial growth [17]. AX3 (parental line for *cln3*$^-$ cells) was used as the WT cell line. *cln3*$^-$ cells also required blasticidin S hydrochloride (10 μg/ml) [18]. Cells in the mid-log phase of growth (1–5 × 10^6 cells/ml) were used for all experiments. HL5 and FM were purchased from Formedium (Hunstanton, Norfolk, UK). KK2 buffer was composed of 2.2 g/l KH_2PO_4 and 0.7 g/l K_2HPO_4, pH 6.5. Mouse monoclonal anti-β-actin was purchased from Santa Cruz Biotechnology Incorporated (Santa Cruz, California, USA). Rabbit polyclonal anti-AprA [19], rabbit polyclonal anti-CfaD [20], rabbit polyclonal anti-CmfA [21], and rabbit polyclonal anti-CtnA [22] were generously provided as gifts by Dr. Richard Gomer (Texas A&M University). The substrate for human TPP1/CLN2, L-alanine-L-alanine-L-phenylalanine-7-amido-4-methylcoumarin, was purchased from Santa Cruz Biotechnology Incorporated (Santa Cruz, California, USA). The substrate for cathepsin D (CTSD)/CLN10, benzoyl-L-arginine-L-glycine-L-phenylalanine-L-phenylalanine-L-proline-4-methoxy-2-naphthylamine (Bz-Arg-Gly-Phe-Phe-Pro-4M2NA) was purchased from Sigma-Aldrich Canada (Oakville, Ontario, Canada). 4-methylumbelliferyl β-d-glucopyranoside (substrate for beta-glucosidase), *p*-nitrophenyl-α-mannoside (substrate for alpha-mannosidase), and 4-nitrophenyl-*N*-acetyl-β-D-glucosaminide (substrate for *N*-acetylglucosamine) were purchased from Sigma-Aldrich Canada (Oakville, Ontario, Canada). 2-N-morpholinoethanesulfonic acid (MES) buffer was purchased from Fisher Scientific Company (Ottawa, Ontario, Canada). The Griess reagent system was purchased from Promega Corporation (Madison, Wisconsin, USA). All statistical analyses were performed in GraphPad Prism 6 (GraphPad Software Incorporated, La Jolla, California, USA).

2.2. Storage body accumulation assay

Cells (5 × 10^5 cells/ml) were incubated in low fluorescence HL5 for 2 h. Cells were also starved for 6 h in KK2 buffer. Aliquots of growth-phase and starved cells (50 μl) were then added to separate wells of a 96-well black clear-bottom plate. Autofluorescence due to storage body accumulation was measured using previously reported parameters (excitation: 340–380 nm, emission: 440–480 nm) [23]. As a control, a range where storage bodies do not autofluoresce was also measured (excitation: 475–495 nm, emission: 565–615 nm) [24]. Statistical significance was assessed using the Student's *t*-test.

2.3. Enzyme activity assays

Enzyme assays were performed using a previously described method [25]. Briefly, cells were grown in HL5 overnight to confluency in 60 mm × 15 mm Petri dishes (8 × 10^6 cells total). Growth-phase cells and cells starved for 4 h in KK2 buffer were lysed with NP40 lysis buffer (50 mM Tris HCl pH 8.0, 150 mM NaCl, 0.5% NP-40). Enzyme assays were performed after 4 h of starvation since previous work showed that secreted enzyme activity (including *N*-acetylglucosaminidase, beta-glucosidase, and alpha-mannosidase) increases dramatically at the onset of starvation and then plateaus after 4 h [26–28]. Likewise, intracellular enzyme activity decreases dramatically at the onset of starvation and reaches a low plateau after 4 h [26]. Previous work also reported that enzyme activity in lysosomal enzyme secretion mutants (like *cln3*$^-$) is unstable after 6 h of starvation, and instead, enzyme activity should be measured at earlier time points [27]. For these reasons, we chose to assess enzyme activity after 4 h of starvation. To assay the activity of beta-glucosidase, lysates (10 μl) were added to 75 μl of 8 mM of 4-methylumbelliferyl β-d-glucopyranoside in 10 mM acetate buffer (pH 5.0) [29]. To assay the activity of alpha-mannosidase, lysates (10 μl) were added to separate wells of a 96-well black clear-bottom plate that contained 75 μl of 8 mM of *p*-nitrophenyl-α-mannoside in 10 mM acetate buffer (pH 5.0). Plates were then incubated for 20 min at 35 °C after which time 75 μl of 1 M Na_2CO_3 was deposited into the wells to stop the reactions. The amount of cleaved substrate was measured using a BioTek Synergy HT microplate reader (BioTek Instruments Incorporated, Winooski, Vermont, USA). 4-methylumbelliferyl β-d-glucopyranoside (substrate for beta-glucosidase) was measured at an excitation of 365 nm and an emission of 445 nm. *p*-nitrophenyl-alpha-mannoside (substrate for alpha-mannosidase) was measured at 405 nm. Previously reported methods were used to measure the activity of Tpp1 and CtsD, with minor modifications [30,31]. To assess Tpp1 activity, lysates (50 μl) were first added to L-Alanyl-L-alanyl-L-phenylalanine 7-amido-4-methylcoumarin (50 μl) dissolved in 100 mM sodium acetate buffer (pH 3.8). Reactions were then incubated in the dark at room temperature for 30 min and then quenched by adding 75 μl of 1 M Na_2CO_3. Samples were analyzed using a BioTek Synergy HT microplate reader (excitation: 365 nm, emission: 445 nm) (BioTek Instruments Incorporated, Winooski, Vermont, USA). To assess CtsD activity, lysates (10 μl) were added to Bz-Arg-Gly-Phe-Phe-Pro-4M2NA (50 μl, 50 μM) dissolved in 50 mM citrate buffer (pH 4.2). Reactions were incubated at 37 °C for 1 h and then quenched by adding 240 μl of 20% trichloroacetic acid. Fluorescence was measured as described above. Statistical significance was assessed using the one-sample *t*-test.

2.4. Endo-lysosomal pH assay

Endo-lysosomal pH was measured using a modified protocol based on previously described methods [32–35]. Cells in the mid-log phase of growth (1–5 × 10^6 cells/ml) were re-suspended in 5 ml of fresh HL5 to a final concentration of 5 × 10^6 cells/ml. This cell suspension was incubated at 150 rpm for 15 min, after which time 100 μl of FITC-dextran (100 mg/ml) was added to the 5 ml culture (2 mg/ml final concentration of FITC-dextran). Cells were incubated with FITC-dextran for 3 h at 150 rpm, after which time 500 μl aliquots were removed and added to separate tubes containing 1 ml ice-cold HL5. Cells were washed one time with ice-cold HL5 and then resuspended in 500 μl of room temperature HL5. At the indicated time points (0, 15, 30, 45, 60, 75, 90 min), cells in HL5 were spun down and washed two times with ice-cold 50 mM MES buffer. The final pellet was resuspended in 500 μl of

500 mM MES buffer and a 100 µl aliquot was then removed for flourimetric analysis using a BioTek Synergy HT microplate reader (BioTek Instruments Incorporated, Winooski, Vermont, USA). Two fluorescence readings were obtained for each sample: 1. Excitation at 400 ± 30 nm and Emission at 528 nm, 2. Excitation at 505 ± 25 nm and Emission at 528 nm. The ratio of fluorescence at the two excitations (I_{505}/I_{400}) is proportional to the endo-lysosomal pH [35]. After accounting for background fluorescence, fluorescence ratios for individual samples were calculated. The endo-lysosomal pH was determined by referencing a standard curve that was generated using FITC-dextran (10 µg/ml) in 500 mM MES buffer at various pH ranging from 4.0 to 8.0. Statistical significance was assessed using two-way ANOVA followed by Bonferroni's multiple comparisons test.

2.5. Nitrite oxide assay

Levels of nitric oxide (NO) were measured using the Griess reagent system and a method previously described [36]. The Griess reagent system provides an indirect measurement of NO by measuring the concentration of nitrite within samples (breakdown product of NO) [37]. Growth-phase cells (1×10^6 total) were harvested from suspension and deposited in Petri dishes containing HL5. After 1 h, the HL5 was removed and cells were washed with KK2 buffer. Confluent cells were incubated in KK2 buffer for 12 h and samples of conditioned KK2 buffer were harvested every 4 h. Absorbance was measured using a BioTek Synergy HT microplate reader at 520 nm (BioTek Instruments Incorporated, Winooski, Vermont, USA). While nitrite was not detected in KK2 buffer, a blank measurement was performed (KK2 buffer only) prior to taking readings of the conditioned buffer to account for any background fluorescence. Statistical significance was assessed using two-way ANOVA followed by Bonferroni's multiple comparisons test.

2.6. SDS-PAGE and western blotting

Cells (5×10^6) grown axenically in HL5 were deposited in 6-well dishes. Growth-phase cells and cells starved for 6 h in phosphate buffer were harvested and lysed. Proteins (5 µg) were separated by SDS-PAGE and analyzed by western blotting with anti-AprA (1:1000), anti-CfaD (1:1000), anti-CMF (1:1000), anti-countin (1:1000), or anti-actin (1:1000) (loading control). Protein levels were quantified using Fiji/ImageJ and normalized against the level of actin at the relevant time point. Statistical significance was assessed using the one-sample *t*-test.

2.7. Preparation of RNA

Cells (5×10^6 total) grown in HL5 and in the mid-log phase of growth (1–5 $\times 10^6$ cells/ml) were deposited into separate wells of a 6-well dish and submerged in HL5. After 3 h, the HL5 was removed from all wells. In one set of wells, the cells were submerged in fresh HL5 for 6 h at room temperature. In another set of wells, the cells were washed one time with KK2 buffer, and then submerged in fresh KK2 buffer for 6 h at room temperature. After 6 h, the media/buffer was removed from the wells. Cells were harvested and washed one time with KK2 buffer. Total RNA was extracted immediately from cells using the RNeasy Plus Mini Kit (Qiagen Incorporated, Toronto, Ontario, Canada). RNA was flash-frozen in liquid nitrogen and stored at −80 °C for future use. Three biological replicates were harvested for each experimental condition.

2.8. RNA sequencing and bioinformatic analyses

RNA sequencing (RNA-seq) was performed by the Centre for Applied Genomics at the Hospital for Sick Children (Toronto, Ontario, Canada). Detailed methods used to generate the RNA-seq datasets are provided in the Supplementary Methods (Methods S1). GO term enrichment analyses were performed using LAGO (A Logically Accelerated GO Term Finder) [38]. A p-value cut-off of 0.05 and the Bonferroni correction were applied for all GO term enrichment analyses. Genes that were upregulated during starvation in *cln3*$^-$ cells compared to WT (205 total, Table S1) were further analyzed by STRING (database version 10.5, https://string-db.org/) [39]. STRING compiles data from homologs in over 2000 organisms to generate a network between the encoded proteins based on direct (e.g., binding) and indirect interactions (e.g., function in a similar metabolic pathway or process) [39]. The downregulated genes were not analyzed by STRING since we found this analysis to be most informative when connecting 100–300 genes.

3. Results

3.1. Differential gene expression in *cln3*$^-$ cells during growth and starvation

Our previous work suggested a role for Cln3 in protein secretion, adhesion, and aggregation during the first 6 h of multicellular development [7,8,9]. Based on these findings, we performed RNA-seq on 6 h starved cells to explore the mechanisms underlying these *cln3*-deficiency phenotypes. Only those genes that were differentially expressed or repressed at least 2-fold and with a false discovery rate (FDR) ≤ 0.05 were included in the analysis (i.e., $\log_2$ fold change values between −1 and 1 were excluded from the analysis). During growth, 54 genes (including *cln3*) were differentially expressed in *cln3*$^-$ cells compared to WT, while 1166 genes (including *cln3*) were differentially expressed during starvation (Table 1, Table S1). A total of 12 genes (excluding *cln3*) were differentially expressed in both conditions. As a result, 1153 genes (excluding *cln3*) were differentially expressed only during starvation. GO term enrichment analyses were performed on the differentially expressed genes using LAGO (A Logically Accelerated GO Term Finder) [38]. Prior to this analysis, unannotated genes were removed from each dataset to prevent these genes from skewing our analysis. This was done by inputting the list of differentially expressed genes for each experimental condition into LAGO (53 genes for growth and 1153 genes for starvation), which identified genes that had GO terms associated with them for each category (e.g., biological process, molecular function, cellular component). The annotated genes were subsequently used for GO term enrichment analysis. During growth, there was no enrichment of GO terms associated with genes differentially expressed in *cln3*$^-$ cells compared to WT. However, during starvation, genes differentially expressed in response to *cln3*-deficiency are primarily linked to metabolic and biosynthetic processes (Table S2). In addition, the differentially expressed genes encode proteins that are involved in some form of binding (e.g., ion, carbohydrate-derivative, ATP) and have catalytic activity (e.g., hydrolase, transferase, lysozyme, cysteine-type endopeptidase) (Table S2). Finally, the proteins encoded by the differentially expressed genes localize to the nucleus and mitochondrion, as well as the cytoplasm, cell periphery, plasma membrane (e.g., integral component of membrane), and extracellular space (Table S2). The localization of proteins to the cell periphery, plasma membrane, and extracellular space is consistent with the role of Cln3 in regulating protein secretion in *Dictyostelium* [7,8].

We also analyzed the enrichment of GO terms associated with either downregulated or upregulated genes during starvation. In terms of biological process, downregulated genes are primarily involved in metabolic and biosynthetic processes (e.g., macromolecule metabolic process) (Table S3). In contrast, upregulated genes are primarily linked to development (e.g., developmental process, sporulation), which is consistent with the precocious development of *cln3*$^-$ cells (Table S3) [7]. In terms of molecular function, both downregulated and upregulated genes encode proteins that are involved in some form of binding and have catalytic activity (Table S3). The proteins encoded by downregulated genes localize to the nucleus, mitochondrion, cytoplasm, cell periphery, and plasma membrane (e.g., integral component of membrane) (Table S3). There was also an enrichment of genes

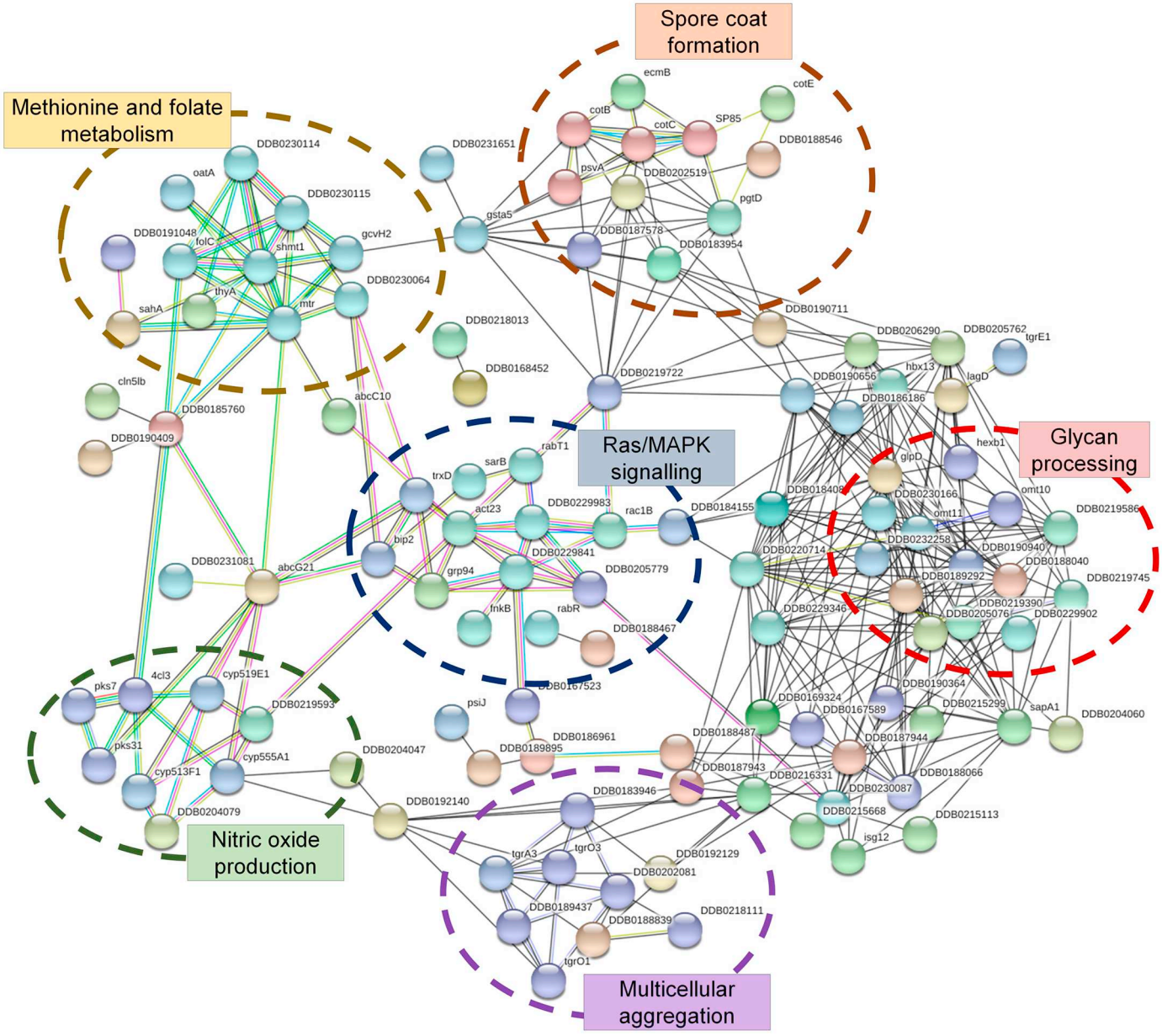

Fig. 1. STRING analysis of genes upregulated in *cln3*$^{-}$ cells compared to WT during starvation. Interactions are represented by lines that connect the nodes (i.e., genes). Interactions were included if they were above the medium confidence threshold (default setting) for the interaction sources.

encoding proteins that localize outside of the cell (e.g., extracellular region), which is consistent with the role of Cln3 in regulating protein secretion in *Dictyostelium* (Table S3) [7,8]. In contrast, upregulated genes only showed an enrichment of proteins that localize to membranes (e.g., intrinsic component of membrane) (Table S3).

Genes that were upregulated in *cln3*$^{-}$ cells during starvation were also analyzed by STRING (205 total, Table S1). STRING compiles data from homologs in over 2000 organisms to generate a protein interaction network [39]. The central pathway connecting the upregulated genes is the Ras/MAPK signalling pathway (Fig. 1). Genes upregulated during starvation in response to *cln3*-deficiency are also linked to glycan processing, methionine and folate metabolism, NO production, multicellular aggregation, and spore coat formation (Fig. 1). The downregulated genes were not analyzed by STRING since the dataset was too large for this type of analysis. However, RNA-seq did reveal downregulated genes that are consistent with our understanding of CLN3 function in other systems. For example, membrane fluidity is altered in cells derived from *CLN3*-deficient mice and therapeutic targeting of the altered fluidity reverses *CLN3*-deficiency phenotypes [40,41]. This phenotype has been linked to the abnormal trafficking of proteins such as caveolin-1, syntaxin-6, and multidrug resistance protein 1, which comprise microdomains in mammalian cells [41]. Two of the three proteins, syntaxin-6 and multidrug resistance protein 1, have putative homologs in *Dictyostelium*, which are encoded by *syn6* and *tagA*, respectively. Also, in mammalian cells, syntaxin-6 interacts with the conserved oligomeric Golgi (COG) complex to positively regulate endosome to trans-Golgi network (TGN) retrograde transport [42]. Intriguingly, RNA-seq revealed that *syn6* (DDB_G0284185), *tagA* (DDB_G0293002), and *cog7* (DDB_G0286705) are all downregulated in *cln3*$^{-}$ cells during starvation, which is consistent with the role of Cln3 in regulating protein trafficking and secretion in *Dictyostelium* [7,8] (Table S1).

3.2. Using comparative transcriptomics to explore the effect of cln3-deficiency on protein secretion, adhesion, aggregation, and osmoregulation

During the growth phase of the *Dictyostelium* life cycle, cell proliferation is modulated by autocrine proliferation repressor A (AprA) [19]. Our previous work showed that *cln3*-deficiency alters the secretion and cleavage of AprA, which results in an increased rate of proliferation of *cln3*$^-$ cells [7]. Loss of *cln3* also increases the secretion of AprA during starvation, which is important considering that AprA also functions as a chemorepellent during the early stages of multicellular development [8,43]. In this study, *cln3*-deficiency reduced the expression of *aprA* (DDB_G0281663) in cells starved for 6 h (Table S1). Consistent with these findings, we observed significantly less AprA protein in *cln3*$^-$ cells starved for 6 h compared to WT cells (Fig. 2). Pull-down assays suggest that AprA interacts with counting factor associated protein D (CfaD), which like AprA, functions extracellularly to repress cell proliferation in *Dictyostelium* [20]. However, there was no effect of *cln3*-deficiency on the expression of *cfaD* or the amount of CfaD protein in cells starved for 6 h (Table S1, Fig. 2). Aggregation during the early stages of *Dictyostelium* development is regulated by several secreted proteins. Two of the most well-studied proteins that regulate this process are conditioned media factor (CmfA) and countin (CtnA) [44,45]. CmfA is a cell-density glycoprotein that modulates the response of cells to pulses of cAMP [45]. CtnA is a component of the 450-kDa counting factor (CF) complex that negatively regulates aggregate size and cell adhesion [44]. While there was no effect of *cln3*-deficiency on *cmfA* expression, the expression of *ctnA* (DDB_G0274597) was significantly reduced in *cln3*$^-$ cells compared to WT cells after 6 h of starvation (Table S1). Consistent with these findings, the amount of CtnA protein, but not CmfA protein, was reduced in *cln3*$^-$ cells starved for 6 h (Fig. 2). Together, these data show that the reduced expression of *aprA* and *ctnA* in *cln3*$^-$ cells during starvation correlates with reduced levels of AprA and CtnA protein. These findings provide strong support for our differential expression analysis and suggest that the altered expression of these two proteins, which function during the early stages of multicellular development, may play a role in the reduced adhesion and delayed aggregation of *cln3*$^-$ cells [9].

Our previous work revealed that *cln3*-deficiency de-regulates protein secretion, reduces adhesion, delays aggregation, and alters osmoregulation [7,8,9,11]. To gain additional insight into the mechanisms underlying these phenotypes, we examined the GO term enrichment analysis of genes differentially expressed in *cln3*$^-$ cells to identify specific genes linked to each of these cellular processes. In *Dictyostelium*, loss of *cln3* de-regulates protein secretion [7,8]. Our RNA-seq dataset identified four differentially expressed genes that are linked to secretion, including *rab11B* (DDB_G0287211), vacuolin B (*vacB*, DDB_G0279191), and vacuole membrane protein 1 (*vmp1*, DDB_G0285175) (Table 2). The Vmp1 protein is linked to a variety of processes in *Dictyostelium* including autophagy, exocytosis, cell proliferation, aggregation, Golgi organization, and the biogenesis of the contractile vacuole (CV) system during osmotic stress [46–48]. Notably, there is evidence linking the function of Cln3 in *Dictyostelium* to each of these processes [7–9,11]. *cln3*-deficiency also reduces cell-substrate and cell-cell adhesion during the early stages of development, which delays aggregation [9]. Seven genes linked to adhesion were differentially expressed in *cln3*$^-$ cells, including countin-1 (*ctnA*, DDB_G0274597) and countin-2 (*ctnB*, DDB_G0279797) (Table 2). Also, 16 genes linked to aggregation were differentially expressed in *cln3*$^-$ cells, including *aprA* (DDB_G0281663), *vmp1* (DDB_G0285175), and ABC transporters (Table 2). Finally, previous work revealed that loss of *cln3* alters the ability of cells to respond to osmotic stress [11]. Nine genes linked to osmoregulation were differentially expressed during starvation, including P2X receptor C (*p2xC*, DDB_G0275191), *vmp1* (DDB_G0285175), and an ABC transporter (*abcG21*, DDB_G0269206) (Table 2). In total, this analysis identified several genes that are linked to specific *cln3*-deficiency phenotypes in *Dictyostelium*.

Table 1
Number of differentially expressed genes in *cln3*$^-$ cells compared to WT during growth and starvation (*cln3* included) (FDR ≤ 0.05).

Experimental condition	Total number of genes	Downregulated genes	Upregulated genes
Growth	54	23	31
Starvation	1166	955	211

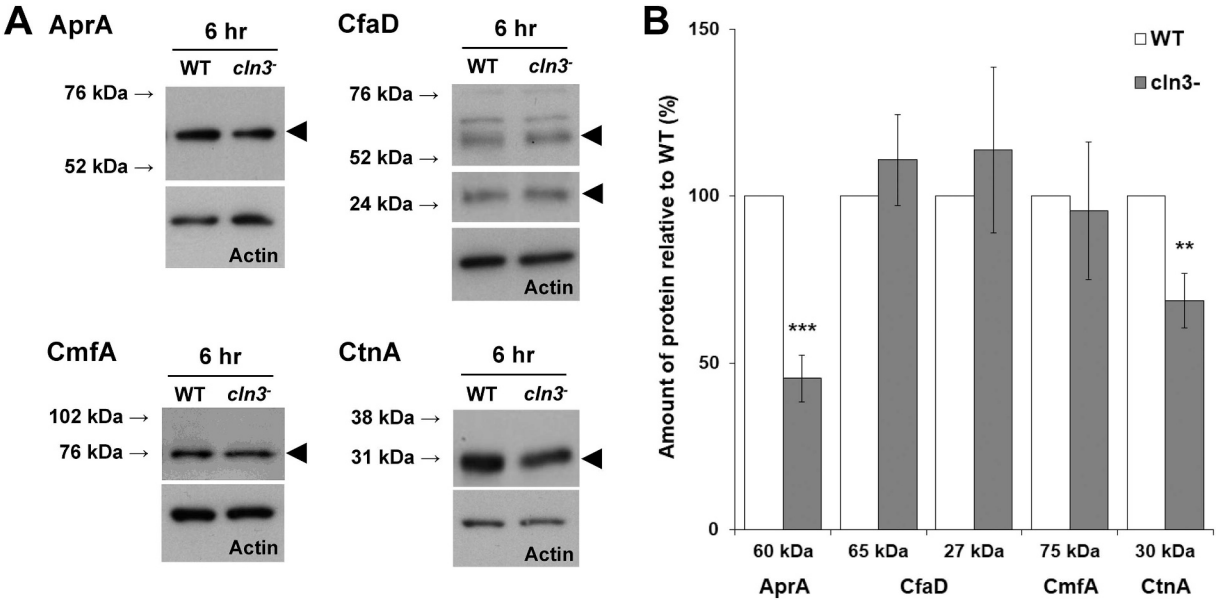

Fig. 2. Intracellular levels of AprA, CfaD, CmfA, and CtnA during starvation. (A) WT and *cln3*$^-$ cells were starved in KK2 buffer for 6 h, after which time the cells were lysed. Whole cell lysates (5 μg) were separated by SDS-PAGE and analyzed by western blotting with anti-AprA, anti-CfaD, anti-CmfA, anti-CtnA, and anti-actin (loading control). Molecular weight markers (in kDa) are shown to the left of each blot. (B) Quantification of the intracellular levels of AprA, CfaD, CmfA, and CtnA. Protein levels were normalized against the level of actin. Data presented as mean amount of protein relative to WT (%) ± SEM (n = 8). **p < .01. ***p < .001.

Table 2
List of differentially expressed genes linked to *cln3*-deficiency phenotypes in *Dictyostelium*.

Secretion (GO:0032940, secretion by cell; GO:0046903, secretion)

UniProt ID	dictyBase ID	Protein names	Gene names	logFC
Q54WZ2	DDB_G0279191	Vacuolin-B	vacB DDB_G0279191	−1.59
Q54NL4	DDB_G0285175	Vacuole membrane protein 1 homolog (Transmembrane protein 49 homolog)	vmp1 tmem49 DDB_G0285175	−1.33
Q55DR2	DDB_G0270556	Uncharacterized protein	DDB0201760	−1.11
Q54KM9	DDB_G0287211	Ras-related protein Rab-11B	rab11B DDB_G0287211	−1.07

Adhesion (GO:0098609, cell-cell adhesion; GO:0007155, cell adhesion; GO:0022610, biological adhesion)

UniProt ID	dictyBase ID	Protein names	Gene names	logFC
Q8WSR7	DDB_G0279797	Countin-2	ctnB DDB_G0279797	−2.12
Q86HE5	DDB_G0269248	Counting factor 45–1	cf45–1 ctnC DDB_G0269248	−2.00
Q86IW0	DDB_G0274779	Uncharacterized protein	DDB0217468	−1.74
Q55C60	DDB_G0270214	Uncharacterized protein	DDB0190882	−1.72
Q86IV5	DDB_G0274597	Countin-1	ctnA DDB_G0274597	−1.48
Q58A40	DDB_G0270212	Uncharacterized protein	DD7–1 DDB0190881	−1.41
Q55BG3	DDB_G0271320	Uncharacterized protein csb family protein DDB_G0271320	DDB_G0271320	−1.15

Aggregation (GO:0098743, cell aggregation; GO:0098630, aggregation of unicellular organisms; GO:0031152, aggregation involved in sorocarp development)

UniProt ID	dictyBase ID	Protein names	Gene names	logFC
Q8WSR7	DDB_G0279797	Countin-2	ctnB DDB_G0279797	−2.12
Q86HE5	DDB_G0269248	Counting factor 45–1	cf45–1 ctnC DDB_G0269248	−2.00
Q5XM24	DDB_G0281663	Autocrine proliferation repressor protein A (PhoPQ-activated pathogenicity-related protein)	aprA DDB_G0281663	−1.63
Q86IV5	DDB_G0274597	Countin-1	ctnA DDB_G0274597	−1.48
Q54NL4	DDB_G0285175	Vacuole membrane protein 1 homolog (Transmembrane protein 49 homolog)	vmp1 tmem49 DDB_G0285175	−1.33
Q54ET0	DDB_G0291356	Metabotropic glutamate receptor-like protein E (DdmGluPR) (GABA-B receptor-like protein grlE)	grlE GluPR DDB_G0291356	−1.28
Q55DR1	DDB_G0269210	ABC transporter G family member 14 (ABC transporter ABCG.14)	abcG14 DDB_G0269210	−1.26
Q86A02	DDB_G0275635	Uncharacterized protein	PIPkinA DDB0185056	−1.16
A2V850	DDB_G0289521	Starvation responsive small protein (Starvation responsive small protein A)	srsA DDB_G0289521	−1.06
Q55GB1	DDB_G0267432	ABC transporter G family member 15 (ABC transporter ABCG.15)	abcG15 DDB_G0267432	−1.02
P15270	DDB_G0277141	Spore coat protein SP60	cotC SP60 DDB_G0277141	1.17
P13773	DDB_G0273533	Cyclic AMP receptor 1 (cAMP receptor 1)	carA-1 car1 DDB_G0273397; carA-2 car1 DDB_G0273533	1.21
Q9U8Q1	DDB_G0286825	Tiger protein D1 (Loose aggregate C2 protein) (Loose aggregate D1 protein) (Transmembrane, IPT, Ig, *E*-set, Repeat protein D1)	tgrD1 lagC2 lagD lagD1 DDB_G0286825	1.25
Q8T673	DDB_G0269206	ABC transporter G family member 21 (ABC transporter ABCG.21)	abcG21 abcG13 DDB_G0269206	1.26
P34145	DDB_G0268622	Rho-related protein rac1B	rac1B DDB_G0268622	2.40
Q54V32	DDB_G0280547	GATA zinc finger domain-containing protein 2 (Communication mutant protein H)	comH gtaB DDB_G0280547	4.13

Osmoregulation (GO:0006972, hyperosmotic response; GO:0006970, response to osmotic stress)

UniProt ID	dictyBase ID	Protein names	Gene names	logFC
B0G108	DDB_G0274237	DUF614 family protein	DDB_G0274237	−2.10
Q553Y0	DDB_G0275191	P2X receptor C (P2XC)	p2xC DDB_G0275191	−1.69
Q54CH1	DDB_G0292924	Arrestin domain-containing protein A	adcA DDB_G0292924	−1.49
Q54NL4	DDB_G0285175	Vacuole membrane protein 1 homolog (Transmembrane protein 49 homolog)	vmp1 tmem49 DDB_G0285175	−1.33
Q55E30	DDB_G0269418	Osmotically inducible family protein	DDB_G0269418	1.17
Q8T673	DDB_G0269206	ABC transporter G family member 21 (ABC transporter ABCG.21)	abcG21 abcG13 DDB_G0269206	1.26
Q54FW5	DDB_G0290563	Putative calcium up-regulated protein H	cupH DDB_G0290563	1.27
Q6TMJ3	DDB_G0269254	SrfA-induced gene J protein	sigJ DDB_G0269254	1.43
Q86JP5	DDB_G0271980	Ras-related protein RabR	rabR DDB_G0271980	1.59

3.3. Effect of cln3-deficiency on the expression of homologs of human NCL genes

Work in *Dictyostelium* and other systems suggests that NCL proteins participate in shared or convergent biological pathways [8,11,29,49–55]. Consistent with these findings, loss of *cln3* reduced the expression of genes homologous to the human NCL genes *TPP1/CLN2* (*tpp1D*, DDB_G0287357; *tpp1F*, DDB_G0281823), cathepsin D (*CTSD/CLN10*) (*ctsD*, DDB_G0279411), progranulin (*PGRN/CLN11*) (*grn*, DDB_G0283671), and cathepsin F (*CTSF/CLN13*) (*cprD*, DDB_G0278721; *cprF*, DDB_G0279185; *cprG*, DDB_G0279187; DDB_G0291191, DDB0219654) (Table 3). In addition, the *Dictyostelium* genome encodes four proteins that share sequence similarity with human CLN5 [29]. The function of the protein encoded by the most highly expressed gene, *cln5*, has been characterized [29,51]. In this study, loss of *cln3* increased the expression of one of the other *CLN5*-like genes (*cln5lb*, DDB_G0279757) (Table 3). Together, these findings provide additional evidence linking NCL genes to a shared or convergent biological pathway.

Based on the above findings, we then assessed the activity of Tpp1

Table 3
Effect of *cln3*-deficiency on the expression of genes homologous to human NCL genes.

UniProt ID	dictyBase ID	Gene name	Log2FC	Human gene
Q54KG5	DDB_G0287357	*tpp1D*	−1.70	*TPP1/CLN2*
Q54TD0	DDB_G0281823	*tpp1F*	−2.13	*TPP1/CLN2*
Q54WC3	DDB_G0279757	*cln5lb*	1.45	*CLN5*
O76856	DDB_G0279411	*ctsD*	−1.21	*CTSD/CLN10*
Q54QR7	DDB_G0283671	*grn*	−1.12	*PGRN/CLN11*
P54639	DDB_G0278721	*cprD*	−1.77	*CTSF/CLN13*
Q94503	DDB_G0279185	*cprF*	−1.40	*CTSF/CLN13*
Q94504	DDB_G0279187	*cprG*	−1.82	*CTSF/CLN13*
Q54F16	DDB_G0291191	Uncharacterized	−1.10	*CTSF/CLN13*

and CtsD in *cln3*$^-$ cells during growth and starvation. There was no effect of *cln3*-deficiency on Tpp1 or CtsD activity during growth, which was expected since there was no effect of *cln3*-deficiency on the expression of *tpp1* or *ctsD* during this stage of the life cycle (Fig. S1). Interestingly, despite the reduced expression of *tpp1D* and *tpp1F* in *cln3*$^-$ cells during starvation, we observed increased activity of Tpp1 in *cln3*$^-$ whole cell lysates and conditioned starvation buffer (Table 3, Fig. 3). Consistent with the reduced expression of *ctsD* in *cln3*$^-$ cells during starvation, we observed decreased activity of CtsD in whole cell lysates (Table 3, Fig. 3). Also, CtsD activity was elevated in conditioned starvation buffer harvested from *cln3*$^-$ cells (Fig. 3). In total, these findings provide additional evidence linking the function of Cln3 to Tpp1 and CtsD in *Dictyostelium*.

3.4. Effect of cln3-deficiency on the expression and activity of lysosomal enzymes during starvation

Previous work revealed that lysosomal enzymes are aberrantly secreted by *cln3*$^-$ cells during starvation [8]. Based on these findings, we coupled the RNA-seq dataset with enzymatic assays to examine the expression and activity of lysosomal enzymes in *cln3*$^-$ cells. Loss of *cln3* decreased the expression of *N*-acetylglucosaminidase (*nagA*, DDB_G0287033), beta-glucosidase (*gluA*, DDB_G0292810), and alpha-mannosidase (DDB_G0292918) during starvation (Table S1). Consistent with these findings, the activity of beta-glucosidase and alpha-mannosidase was reduced in *cln3*$^-$ whole cell lysates compared to WT (Fig. 3). However, there was no effect of *cln3*-deficiency on *N*-acetylglucosaminidase activity (Fig. 3). In conditioned starvation buffer harvested from *cln3*$^-$ cells, we observed increased activity of beta-glucosidase, alpha-mannosidase, and *N*-acetylglucosaminidase (Fig. 3). There was no effect of *cln3*-deficiency on the activity of these enzymes during growth, which was expected since there was no effect of *cln3*-deficiency on the expression of these enzymes during this stage of the life cycle (Fig. S1). In total, these findings support a role for Cln3 in the expression, activity, and secretion of lysosomal enzymes during starvation.

3.5. Loss of cln3 reduces the expression of genes encoding V-ATPase subunits, elevates endo-lysosomal pH, and leads to storage body accumulation

Previous work in *Dictyostelium* showed that *cln3*$^-$ cells abnormally secrete V-ATPase subunit D (VatD) during starvation [8]. In this study, the RNA-seq analysis showed that *cln3*-deficiency reduces the expression of genes encoding the V-ATPase subunits *vatA* (DDB_G0287127), *vatC* (DDB_G0284473), and *vatE* (DDB_G0275701) (Table S1). In yeast, loss of the CLN3 homolog Btn1 leads to aberrant assembly of V-ATPase, which alters pH homeostasis [56]. V-ATPase subunit D links the V1 (peripheral) and V0 (membrane-bound) parts of the central rotor [57]. ATP hydrolysis occurs in the V1 region, which then drives proton translocation through the membrane-embedded V0 region via rotation of the rotor [57]. Based on these findings, we wanted to determine if the reduced expression of V-ATPase subunits and the abnormal secretion of VatD in response to *cln3*-deficiency in *Dictyostelium* affected the ability of cells to acidify intracellular compartments. Therefore, we used a well-established assay that measures endo-lysosomal pH during growth. Endo-lysosomal pH was examined during growth since the assay relies on the uptake of FITC-dextran and the progression of the molecule through the endocytic pathway. While we did not observe differential expression of V-ATPase subunits in *cln3*$^-$ cells during growth, we did observe increased expression of *nhe3* (DDB_G0292830) (Table S1). Nhe3 is a transmembrane domain-containing protein that is predicted to regulate pH homeostasis by functioning as a cation/hydrogen exchanger (http://dictybase.org). When we carried out the endo-lysosomal pH assay, we observed that *cln3*$^-$ cells were able to acidify intracellular compartments, but the pH in the compartments was elevated compared to WT cells (Fig. 4A).

Since there is evidence supporting the presence of V-ATPase subunits in lipofuscin deposits found in rat and human brains, we measured the autofluorescent properties of *cln3*$^-$ cells using the same assay that was used to reveal autofluorescent storage bodies in *cln5*$^-$ cells [51,58]. Our analysis revealed an increased amount of autofluorescence in *cln3*$^-$ cells compared to WT cells during starvation, but not during growth (Fig. 4B, Fig. S2). This autofluorescence was observed within a range that is indicative of storage body accumulation in human cells [23]. While autofluorescence was also observed within a control range (i.e., where storage bodies do not autofluoresce in human cells), the intensity of the fluorescence was significantly lower, and there was no effect of *cln3*-deficiency on the levels observed (Fig. 4B, Fig. S2) [24]. Together, these results show that loss of *cln3* affects the expression and localization of V-ATPase subunits. Consequently, this elevates the pH of intracellular compartments and leads to an accumulation of autofluorescent storage bodies in *cln3*$^-$ cells.

3.6. Effect of cln3-deficiency on nitric oxide production

Altered nitrogen metabolism has been reported in yeast and mouse models of CLN3 disease and our RNA-seq analysis revealed 283 differentially expressed genes with the GO term, nitrogen compound metabolic process (GO:0006807) (Table S2) [59–61]. Also, STRING analysis identified a network of upregulated genes linked to NO production (Fig. 1). In fungi, polyketides inhibit NO production [62]. Intriguingly, genes that encode putative polyketide synthases were upregulated in *cln3*$^-$ cells during starvation (*pks7*, DDB_G0271614; *pks31*, DDB_G0290703) (Table S1). To further explore the effect of *cln3*-deficiency on NO homeostasis, we analyzed samples of conditioned starvation buffer using the Griess reagent system, which measures the levels of nitrite (the primary breakdown product of NO) in samples [37]. We analyzed the secreted levels of nitrite since these levels are representative of NO production in *Dictyostelium* and mammalian systems [63,64]. Consistent with previous findings, nitrite accumulated at an expected rate in conditioned starvation buffer from WT cells [36]. However, the levels of nitrite in *cln3*$^-$ conditioned buffer were reduced compared to WT (Fig. 5). In total, these results are consistent with the differential expression of genes linked to nitrogen metabolism in *cln3*$^-$ cells.

4. Discussion

Loss of *cln3* causes several phenotypes during the *Dictyostelium* life cycle including increased cell proliferation, altered osmoregulation, reduced adhesion, aberrant protein secretion, and precocious multicellular development [7–9,11]. In this study, we used RNA-seq to provide transcriptional data that supports previously published findings in *Dictyostelium* and other genetic models of CLN3 disease. The results of the RNA-seq analysis also allowed us to reveal new *cln3*-deficiency phenotypes in *Dictyostelium* including aberrant expression and activity

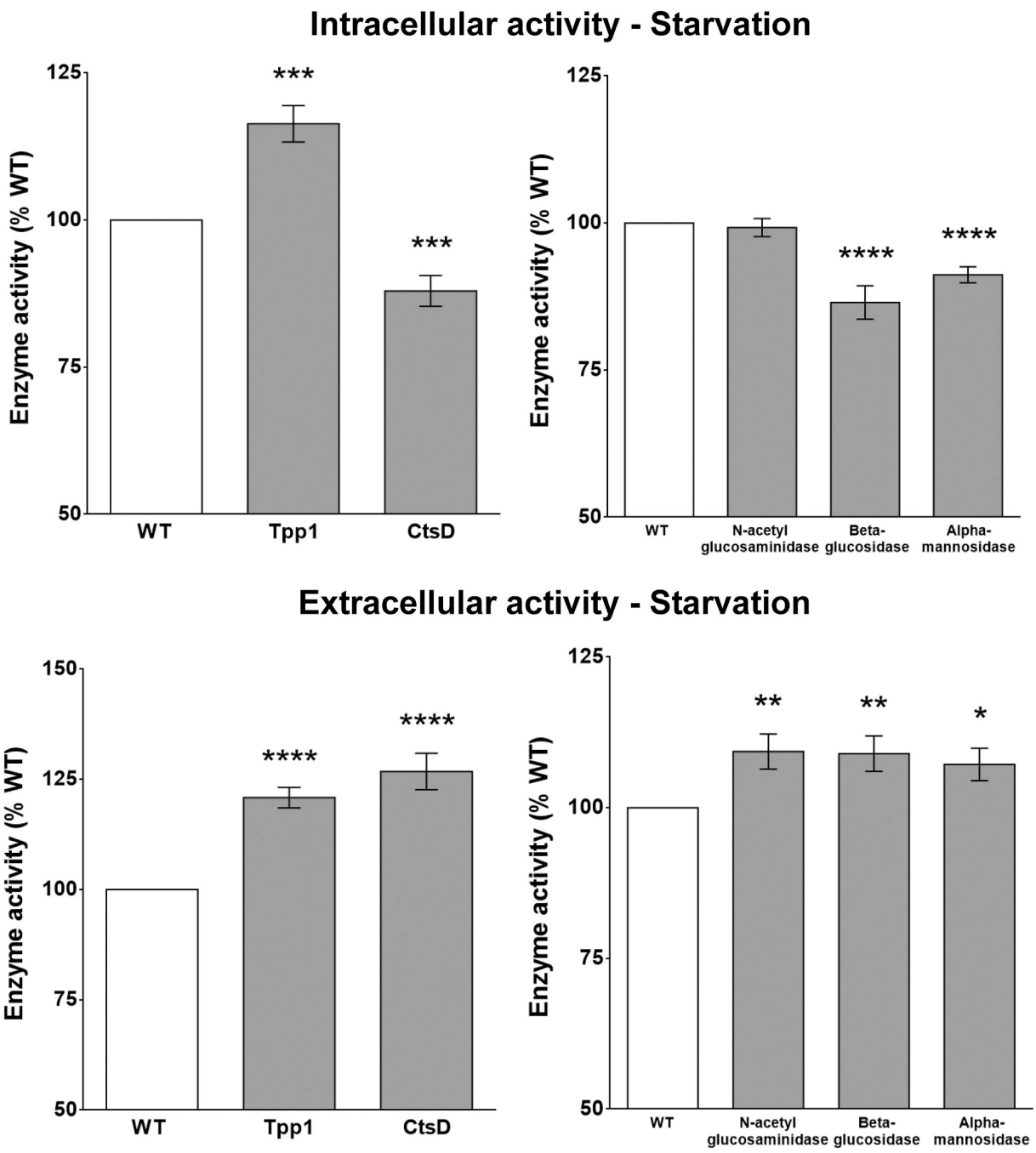

Fig. 3. Effect of *cln3*-deficiency on the activity of Tpp1, CtsD, *N*-acetylglucosaminidase, beta-glucosidase, and alpha-mannosidase during starvation. Cells were starved for 4 h in KK2 buffer, after which time the conditioned buffer was collected and the cells lysed with NP40 lysis buffer. The activities of tripeptidyl peptidase 1 (Tpp1), cathepsin D (CtsD), *N*-acetylglucosaminidase, beta-glucosidase, and alpha-mannosidase were assessed. Data presented as mean enzyme activity (% WT) ± SEM (n = 12–18). *p < .05. **p < .01. ***p < .001. ****p < .0001.

of lysosomal enzymes, increased endo-lysosomal pH, and altered NO homeostasis. We also provide additional evidence linking NCL proteins to a common pathway and show that autofluorescent storage bodies accumulate in *cln3*$^{-}$ cells. In total, this study provides new insight into the function of Cln3 in *Dictyostelium* and sets the stage for future studies to further explore the molecular mechanisms underlying *cln3*-deficiency phenotypes in this model organism.

The RNA-seq dataset suggests that loss of *cln3* alters molecular pathways related to metabolism, biosynthetic processes, and catalysis during starvation. These results are consistent with previous work that reported reduced basal mitochondrial respiration and ATP production in mice harbouring the most common mutation observed in patients with CLN3 disease, and the regulation of CTSD protease activity by CLN3 in baby hamster kidney cells [49,65]. While downregulated genes are linked to metabolic and biosynthetic processes, upregulated genes are primarily linked to development, which is consistent with the precocious development of *cln3*$^{-}$ cells [7]. The RNA-seq analysis also revealed an enrichment of downregulated genes whose protein products localize extracellularly, which supports the aberrant protein secretion observed in *cln3*$^{-}$ cells during starvation [7–9]. In contrast, upregulated genes show an enrichment of proteins that localize to membranes. Interestingly, 40–47% of the genes differentially expressed in *cln3*$^{-}$ cells during growth are unannotated (Table S4). Similarly, 35–39% of the genes differentially expressed during starvation are also

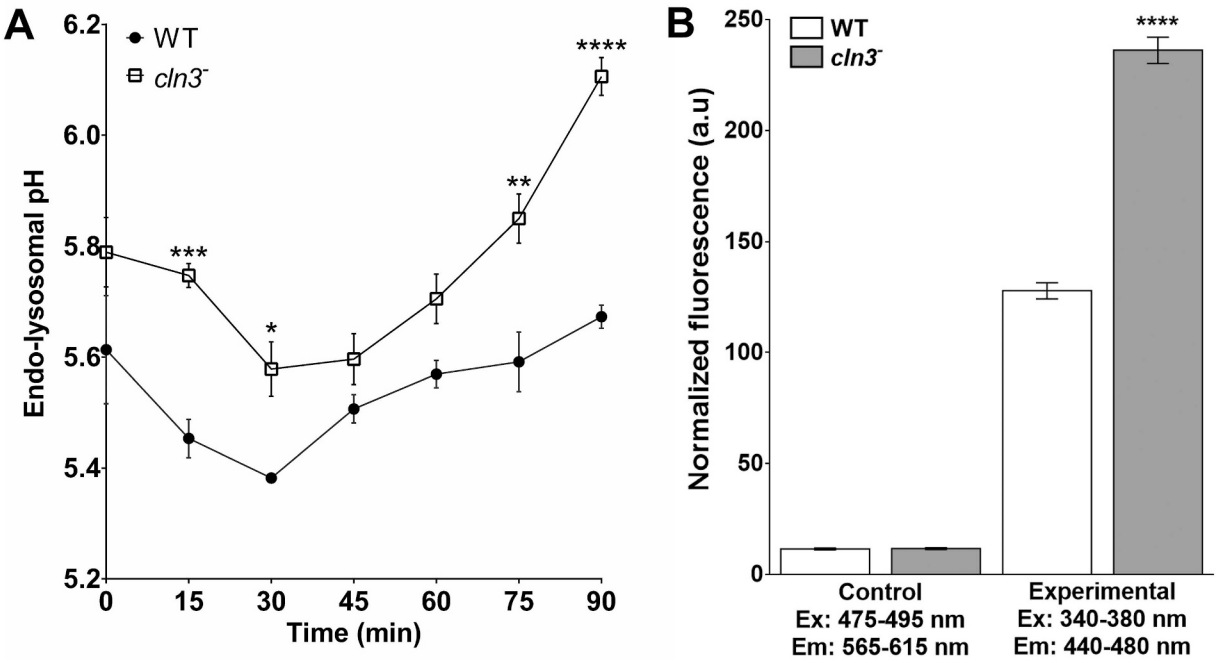

Fig. 4. Effect of *cln3*-deficiency on endo-lysosomal pH and storage body accumulation. (A) Cells were incubated with FITC-dextran for 3 h at 150 rpm, after which time 500 µl of sample was removed, washed with ice-cold HL5, and then resuspended in 500 µl of room temperature HL5. At the indicated times (0, 15, 30, 45, 60, 75, 90 min), cells in HL5 were spun down and washed two times with ice-cold 50 mM MES buffer. The final pellet was resuspended in 1 ml of 500 mM MES buffer and a 100 µl aliquot was then removed for flourimetric analysis. After generating a standard curve and accounting for background fluorescence, the endo-lysosomal pH was calculated (as described in the Materials and Methods). Data presented as mean endo-lysosomal pH ± SEM (n = 4). Statistical significance was determined using two-way ANOVA followed by Bonferonni's multiple comparisons test. *p < .05. **p < .01. ***p < .001. ****p < .0001. (B) Normalized fluorescence in 6 h starved cells captured with a microplate reader. Autofluorescence within a range indicative of storage body accumulation was measured (Experimental, ex: 340–380 nm, em: 440–480 nm). A range where storage bodies do not autofluoresce was also measured (Control, excitation: 475–495 nm, emission: 565–615 nm). Data presented as mean normalized fluorescence ± SEM (n = 14). Statistical significance was assessed using the Student's *t*-test. ****p < .0001.

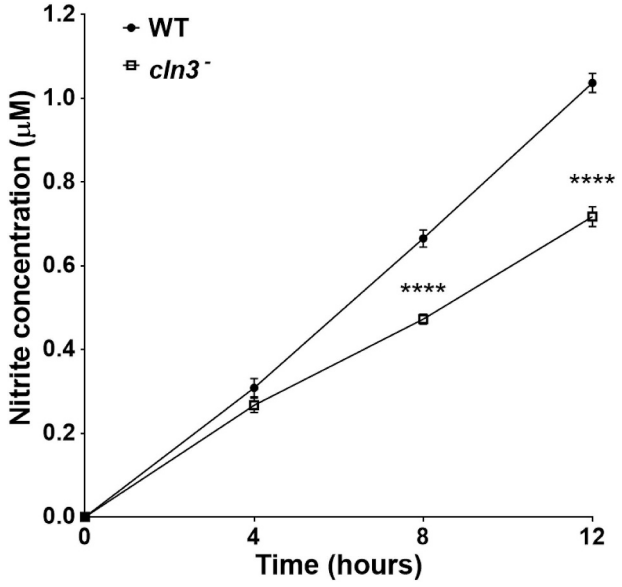

Fig. 5. Effect of *cln3*-deficiency on nitrite production. Conditioned KK2 buffer was collected from starved cells and analyzed using the Griess reagent system. Data presented as mean nitrite concentration ± SEM (n = 9). Statistical significance was determined using two-way ANOVA followed by Bonferroni's multiple comparison test. ****p < .0001.

unannotated (Table S4). Therefore, the future characterization of these genes may reveal additional insight into the molecular mechanisms underlying Cln3 function during growth and starvation in *Dictyostelium*.

The downregulation of *syn6*, *tagA*, and *cog7* in *cln3*$^-$ cells during starvation is consistent with the observations of altered membrane fluidity in mouse models of CLN3 disease [40,41]. Since the aberrant fluidity has been linked to abnormal protein trafficking, these results also support the role of Cln3 in protein trafficking and secretion in *Dictyostelium* [7,8]. Furthermore, there was an enrichment of transmembrane proteins that were upregulated in *cln3*$^-$ cells during starvation, which may reflect a compensatory mechanism in *cln3*-deficient cells to correct possible alterations in membrane fluidity.

STRING analysis revealed networks of upregulated genes that support work in other genetic models of NCL. Genes associated with Ras/MAPK signalling form a central part of the network, which is interesting given that previous work has linked Ras/MAPK signalling to CLN3 disease [66]. The network of genes linked to methionine metabolism supports the presence of *S*-methylated methionine in NCL storage material [67]. Genes linked to glycan processing were also revealed in the STRING analysis, which is consistent with several reports of aberrant glycan processing in mouse and human models of NCL [68–71]. Finally, gene networks linked to NO production, multicellular aggregation, and spore coat formation are supported by previous work in yeast, mouse, and *Dictyostelium* [9,11,59–61].

RNA-seq revealed that *cln3*-deficiency decreases the expression of *aprA* and *ctnA* in starved cells, which correlates with a reduced amount of intracellular AprA and CtnA protein. AprA functions as a chemorepellent during the early stages of multicellular development and CtnA is a component of the 450-kDa CF complex that negatively regulates adhesion and aggregate size [43,44]. Therefore, these results not only provide strong support for the differential expression analysis, but they also indicate that reduced expression of these genes may contribute to the reduced adhesion and delayed aggregation of *cln3*$^-$ cells during the early stages of multicellular development [9].

Previous work in mammalian cells reported molecular interactions

between *CLN3* and other NCL genes including *TPP1/CLN2*, *CLN5*, and *CTSD/CLN10* [49,50,52–55]. In this study, we showed that loss of *cln3* reduced the expression of *tpp1* (*tpp1D*, *tpp1F*), *ctsD*, and genes that share sequence similarity with human *CTSF/CLN13* (*cprD*, *cprF*). Our results also provide the first evidence in any system linking the expression of *cln3* to *grn*, which is interesting given that PGRN has been investigated as a potential therapeutic tool for combating NCL in humans [72,73]. These findings are consistent with our previous work that showed that loss of *cln3* increases the secretion of Tpp1F, Cln5, and CtsD during starvation, and causes aberrant secretion of proteins that are similar to human CTSF/CLN13 (CprA, CprB, CprD, CprE, CprF, CprG) [8]. Our previous work also showed that *Dictyostelium* Cln5 interacts with Tpp1B, CtsD, and uncharacterized protein DDB0252831, which shares sequence similarity with CprA [29]. Together, these data provide strong support for the molecular networking of NCL-like genes in *Dictyostelium*.

Based on the finding that *cln3*-deficiency decreases the expression of *tpp1D, tpp1F,* and *ctsD* during starvation, we assayed Tpp1 and CtsD activity in whole cell lysates and conditioned starvation buffer. Consistent with the reduced expression of *ctsD* in *cln3*$^-$ cells, there was reduced activity of CtsD in starved cells. In addition, CtsD activity was increased in conditioned starvation buffer, which is consistent with previous work that reported increased secretion of CtsD by *cln3*$^-$ cells during starvation [8]. These findings indicate that Cln3 modulates the secretion of CtsD during starvation and loss of *cln3* reduces the expression of *ctsD* due to there being more CtsD outside of the cell (i.e., negative feedback mechanism). While *cln3*-deficiency reduced the expression of *tpp1D* and *tpp1F* during starvation, we observed increased activity of Tpp1 in whole cell lysates and conditioned starvation buffer. This apparent discrepancy can possibly be explained by the relatively low expression of *tpp1D* and *tpp1F* during growth and the early stages of multicellular development. The *Dictyostelium* genome contains six genes that share sequence similarity with human *TPP1* (*tpp1A, tpp1B, tpp1C, tpp1D, tpp1E, tpp1F*) [74]. Of these six genes, *tpp1B* displays the highest expression during growth and the first 6 h of starvation, while *tpp1D* and *tpp1F* are expressed at significantly reduced amounts [75]. Since none of the *tpp1* genes were upregulated in *cln3*$^-$ cells, we reason that loss of *cln3* likely alters the expression of an unidentified interactor that regulates Tpp1 activity in *Dictyostelium*. Finally, previous work in *Dictyostelium* showed that loss of *cln3* increases the secretion of Tpp1F, which could explain the increased activity of Tpp1 in conditioned starvation buffer [8].

Previous work revealed that lysosomal enzymes are aberrantly secreted by *cln3*$^-$ cells during starvation [8]. In this study, GO term enrichment analyses revealed a significant number of differentially expressed genes linked to catalytic activity. More specifically, loss of *cln3* decreased the expression of *N*-acetylglucosaminidase, beta-glucosidase, and alpha-mannosidase in starved cells. As expected, we observed a correlated decrease in beta-glucosidase and alpha-mannosidase activity in whole cell lysates. The decreased expression and activity of beta-glucosidase and alpha-mannosidase inside the cell could possibly be explained by the increased activity of both enzymes outside the cell. Presumably, the increased extracellular activity, which may be a result of over-secretion in response to *cln3*-deficiency, could feed back on the cell to reduce the intracellular expression and activity of beta-glucosidase and alpha-mannosidase (i.e., negative feedback mechanism). While the expression of *nagA* was decreased in *cln3*$^-$ cells, we did not observe an effect of *cln3*-deficiency on the intracellular activity of *N*-acetylglucosaminidase. One reason to explain this observation could be the upregulation of other enzymes that act upon *N*-acetylglucosamine. In fact, our previous work showed that Cln5 is a glycoside hydrolase that cleaves *N*-acetylglucosamine, and in this study, loss of *cln3* increased the expression of one of the other *CLN5*-like genes in *Dictyostelium* (*cln5lb*, DDB_G0279757) [29]. However, in conditioned starvation buffer harvested from *cln3*$^-$ cells, we observed increased *N*-acetylglucosaminidase activity, which is consistent with previous work that showed increased secretion of *N*-acetylglucosaminidase by *cln3*$^-$ cells [8]. Furthermore, *N*-acetylglucosaminidase functions in the ganglioside metabolism pathway and related enzymes of the pathway show altered expression in a mouse model of CLN3 disease [76,77]. Finally, previous work in *Dictyostelium* showed that enzymes secreted during the early stages of development play an important role in facilitating adhesion and aggregation [26,28]. While a subtle change in any one enzyme will likely not significantly affect development, alterations in the expression, activity, and secretion of many enzymes could cause developmental defects. Therefore, it is reasonable to suggest that the aberrant expression, activity, and secretion of enzymes by *cln3*$^-$ cells may be at least partly responsible for the reduced adhesion and delayed aggregation of *cln3*-deficient cells [9].

This study showed that *cln3*-deficiency decreases the expression of genes encoding subunits of the V-ATPase. In addition, previous work showed that *cln3*$^-$ cells secrete the VatD during starvation, which does not normally occur in WT cells [8]. While *cln3*$^-$ cells were able to acidify endocytic compartments, the pH in the compartments was elevated compared to WT cells. These findings are consistent with results from yeast, which show that loss of the CLN3 homolog Btn1 leads to aberrant assembly of V-ATPase and alters pH homeostasis [56]. Since the transcriptional changes indicate that catalytic activity and metabolism are altered in *cln3*$^-$ cells, it is possible that the altered activity of lysosomal enzymes due to elevated lysosomal pH is a contributing factor to these transcriptional changes. Finally, we observed an accumulation of autofluorescent storage bodies in *cln3*$^-$ cells during starvation, which is consistent with previous work that revealed storage body accumulation in *tpp1*$^-$ and *cln5*$^-$ cells [31,51]. The elevated endo-lysosomal pH observed in *cln3*$^-$ cells may have also contributed to the accumulation of this storage material.

Altered nitrogen metabolism has been reported in yeast and mouse models of CLN3 disease [59–61]. In this study, 283 genes linked to nitrogen metabolism were differentially expressed in *cln3*$^-$ cells. STRING analysis of the upregulated genes also revealed a network of genes linked to NO production. Consistent with these findings, we measured lower levels of nitrite in samples of conditioned starvation buffer harvested from *cln3*$^-$ cells. These results adhere to findings from yeast, where loss of *btn1* impairs the synthesis of NO in both physiological and oxidative stress conditions [61]. In addition, genes that encode putative polyketide synthases are upregulated in *cln3*$^-$ cells during starvation, which is noteworthy considering that polyketides inhibit nitric oxide production in fungi [62]. Together, this data indicates that aberrant nitrogen metabolism may play a role in the phenotypes observed in *cln3*$^-$ cells during the early stages of multicellular development.

In summary, this study provides new insight into the function of Cln3 during the early stages of *Dictyostelium* development. We have linked transcriptional changes to cellular and biochemical assays, which enhances our knowledge of the molecular mechanisms underlying Cln3 function in *Dictyostelium*. Further analysis of the genes differentially expressed in *cln3*$^-$ cells during starvation may shed additional insight into the pathways regulating Cln3 function, especially once currently unannotated genes are characterized.

Supplementary data to this article can be found online at https://doi.org/10.1016/j.cellsig.2019.02.004.

Funding

This work was supported by the Canada Foundation for Innovation (to RJH), the Banting Research Foundation (Discovery Award to RJH), and the Natural Sciences and Engineering Research Council of Canada (Discovery Grant to RJH and USRA to SM).

Acknowledgments

We would like to thank Dr. Richard Gomer (Texas A&M University) for generously providing antibodies against AprA, CfaD, CmfA, and CtnA.

References

[1] S.E. Mole, S.L. Cotman, Genetics of the neuronal ceroid lipofuscinoses (batten disease), Biochim. Biophys. Acta 1852 (2015) 2237–2241.
[2] G.W. Anderson, H.H. Goebel, A. Simonati, Human pathology in NCL, Biochim. Biophys. Acta 1832 (2013) 1807–1826.
[3] J. Radke, W. Stenzel, H.H. Goebel, Human NCL neuropathology, Biochim. Biophys. Acta 1852 (2015) 2262–2266.
[4] A. Schulz, A. Kohlschütter, J. Mink, A. Simonati, R. Williams, NCL diseases - clinical perspectives, Biochim. Biophys. Acta 1832 (2013) 1801–1806.
[5] J. Cárcel-Trullols, A.D. Kovács, D.A. Pearce, Cell biology of the NCL proteins: what they do and don't do, Biochim. Biophys. Acta 1852 (2015) 2242–2255.
[6] U. Chandrachud, M.W. Walker, A.M. Simas, S. Heetveld, A. Petcherski, M. Klein, H. Oh, P. Wolf, W.N. Zhao, S. Norton, S.J. Haggarty, E. Lloyd-Evans, S.L. Cotman, Unbiased cell-based screening in a neuronal cell model of batten disease highlights an interaction between Ca2+ homeostasis, autophagy, and CLN3 protein function, J. Biol. Chem. 290 (2015) 14361–14380.
[7] R.J. Huber, M.A. Myre, S.L. Cotman, Loss of Cln3 function in the social amoeba *Dictyostelium discoideum* causes pleiotropic effects that are rescued by human CLN3, PLoS One 9 (2014) e110544.
[8] R.J. Huber, Loss of Cln3 impacts protein secretion in the social amoeba *Dictyostelium*, Cell. Signal. 35 (2017) 61–72.
[9] R.J. Huber, M.A. Myre, S.L. Cotman, Aberrant adhesion impacts early development in a *Dictyostelium* model for juvenile neuronal ceroid lipofuscinosis, Cell Adhes. Migr. 11 (2017) 399–418.
[10] S. Kang, J.H. Seo, T.H. Heo, S.J. Kim, Batten disease is linked to altered expression of mitochondria-related metabolic molecules, Neurochem. Int. 62 (2013) 931–935.
[11] S. Mathavarajah, M.D. McLaren, R.J. Huber, Cln3 function is linked to osmoregulation in a *Dictyostelium* model of batten disease, Biochim. Biophys. Acta 1864 (2018) 3559–3573.
[12] D.J. Metcalf, A.A. Calvi, M.N.J. Seaman, H.M. Mitchison, D.F. Cutler, Loss of the batten disease gene CLN3 prevents exit from the TGN of the mannose 6-phosphate receptor, Traffic 9 (2008) 1905–1914.
[13] J.M. Vidal-Donet, J. Cárcel-Trullols, B. Casanova, C. Aguado, E. Knecht, Alterations in ROS activity and lysosomal pH account for distinct patterns of macroautophagy in LINCL and JNCL fibroblasts, PLoS One 8 (2013) e55526.
[14] S. Mathavarajah, A. Flores, R.J. Huber, *Dictyostelium discoideum*: a model system for cell and developmental biology, Curr. Prot. Ess Lab. Tech. 15 (2017) 14.1.1–19.
[15] S.J. Annesley, S. Chen, L.M. Francione, O. Sanislav, A.J. Chavan, C. Farah, S.W. De Piazza, C.L. Storey, J. Ilievska, S.G. Fernando, P.K. Smith, S.T. Lay, P.R. Fisher, *Dictyostelium*, a microbial model for brain disease, Biochim. Biophys. Acta 1840 (2014) 1413–1432.
[16] R.J. Huber, Using the social amoeba *Dictyostelium* to study the functions of proteins linked to neuronal ceroid lipofuscinosis, J. Biomed. Sci. 23 (2016) 83.
[17] P. Fey, A.S. Kowal, P. Gaudet, K.E. Pilcher, R.L. Chisholm, Protocols for growth and development of *Dictyostelium discoideum*, Nat. Protoc. 2 (2007) 1307–1316.
[18] J. Faix, J. Linkner, B. Nordholz, J.L. Platt, X.H. Liao, A.R. Kimmel, The application of the Cre-loxP system for generating multiple knock-out and knock-in targeted loci, Methods Mol. Biol. 983 (2013) 249–267.
[19] D.A. Brock, R.H. Gomer, A secreted factor represses cell proliferation in *Dictyostelium*, Development 132 (2005) 4553–4562.
[20] D. Bakthavatsalam, D.A. Brock, N.N. Nikravan, K.D. Houston, R.D. Hatton, R.H. Gomer, The secreted *Dictyostelium* protein CfaD is a chalone, J. Cell Sci. 121 (2008) 2473–2480.
[21] R. Jain, R.H. Gomer, A developmentally regulated cell surface receptor for a density-sensing factor in *Dictyostelium*, J. Biol. Chem. 269 (1994) 9128–9136.
[22] D.A. Brock, R.H. Gomer, A cell-counting factor regulating structure size in *Dictyostelium*, Genes Dev. 13 (1999) 1960–1969.
[23] S.K. Jain, K. Abreo, J. Duett, M.L. Sella, Lipofuscin products, lipid peroxides and aluminum accumulation in red blood cells of hemodialyzed patients, Am. J. Nephrol. 15 (1995) 306–311.
[24] A.D. Marmorstein, L.Y. Marmorstein, H. Sakaguchi, J.G. Hollyfield, Spectral profiling of autofluorescence associated with lipofuscin, Bruch's membrane, and sub-RPE deposits in normal and AMD eyes, Invest. Ophthalmol. Vis. Sci. 43 (2002) 2435–2441.
[25] D.H. O'Day, Intracellular and extracellular acetylglucosaminidase activity during microcyst formation in *Polysphondylium pallidum*, Exp. Cell Res. 79 (1973) 186–190.
[26] R.L. Dimond, R.A. Burns, K.B. Jordan, Secretion of lysosomal enzymes in the cellular slime mold, *Dictyostelium discoideum*, J. Biol. Chem. 256 (1981) 6565–6572.
[27] D.L. Ebert, K.B. Jordan, R.L. Dimond, Lysosomal enzyme secretory mutants of *Dictyostelium discoideum*, J. Cell Sci. 96 (1990) 491–500.
[28] E.F. Rossomando, B. Maldonado, E.V. Crean, E.J. Kollar, Protease secretion during onset of development in *Dictyostelium discoideum*, J. Cell Sci. 30 (1978) 305–318.
[29] R.J. Huber, S. Mathavarajah, Cln5 is secreted and functions as a glycoside hydrolase in *Dictyostelium*, Cell. Signal. 42 (2018) 236–248.
[30] J.S. King, A. Gueho, M. Hagedorn, N. Gopaldass, F. Leuba, T. Soldati, R.H. Insall, WASH is required for lysosomal recycling and efficient autophagic and phagocytic digestion, Mol. Biol. Cell 24 (2013) 2714–2726.
[31] J.E. Phillips, R.H. Gomer, Partial genetic suppression of a loss of function mutant of the neuronal ceroid lipofuscinosis-associated protease TPP1 in *Dictyostelium discoideum*, Dis. Model. Mech. 8 (2015) 147–156.
[32] L. Aubry, G. Klein, J.L. Martiel, M. Satre, Kinetics of endosomal pH evolution in *Dictyostelium discoideum* amoebae. Study by fluorescence spectroscopy, J. Cell Sci. 105 (1993) 861–866.
[33] D.T. Brazill, D.R. Caprette, H.A. Myler, R.D. Hatton, R.R. Ammann, D.F. Lindsey, D.A. Brock, R.H. Gomer, A protein containing a serine-rich domain with vesicle fusing properties mediates cell cycle-dependent cytosolic pH regulation, J. Biol. Chem. 275 (2000) 19231–19240.
[34] D.T. Brazill, L.R. Meyer, R.D. Hatton, D.A. Brock, R.H. Gomer, ABC transporters required for endocytosis and endosomal pH regulation in *Dictyostelium*, J. Cell Sci. 114 (2001) 3923–3932.
[35] F. Rivero, M. Maniak, Quantitative and microscopic methods for studying the endocytic pathway, Methods Mol. Biol. 346 (2006) 423–438.
[36] Y. Tao, A. Howlett, C. Klein, Nitric oxide-releasing compounds inhibit *Dictyostelium discoideum* aggregation without altering cGMP production, FEBS Lett. 314 (1992) 49–52.
[37] J. Sun, X. Zhang, M. Broderick, H. Fein, Measurement of nitric oxide production in biological systems by using Griess reaction assay, Sensors 3 (2003) 276–284.
[38] E.I. Boyle, S. Weng, J. Gollub, H. Jin, D. Botstein, J.M. Cherry, G. Sherlock, GO:TermFinder - open source software for accessing gene ontology information and finding significantly enriched gene ontology terms associated with a list of genes, Bioinformatics 20 (2004) 3710–3715.
[39] C. Von Mering, L.J. Jensen, B. Snel, S.D. Hooper, M. Krupp, M. Foglierini, N. Jouffre, M.A. Huynen, P. Bork, STRING: known and predicted protein–protein associations, integrated and transferred across organisms, Nucleic Acids Res. 33 (2005) D433–D437.
[40] M.L. Schultz, L. Tecedor, E. Lysenko, S. Ramachandran, C.S. Stein, B.L. Davidson, Modulating membrane fluidity corrects batten disease phenotypes in vitro and in vivo, Neurobiol. Dis. 115 (2018) 182–193.
[41] L. Tecedor, C.S. Stein, M.L. Schultz, H. Farwanah, K. Sandhoff, B.L. Davidson, CLN3 loss disturbs membrane microdomain properties and protein transport in brain endothelial cells, J. Neurosci. 33 (2013) 18065–18079.
[42] O. Laufman, W. Hong, S. Lev, The COG complex interacts directly with Syntaxin 6 and positively regulates endosome-to-TGN retrograde transport, J. Cell Biol. 194 (2011) 459–472.
[43] J.E. Phillips, R.H. Gomer, A secreted protein is an endogenous chemorepellant in *Dictyostelium discoideum*, Proc. Natl. Acad. Sci. U. S. A. 109 (27) (2012) 10990–10995.
[44] C. Roisin-Bouffay, W. Jang, D.R. Caprette, R.H. Gomer, A precise group size in *Dictyostelium* is generated by a cell-counting factor modulating cell-cell adhesion, Mol. Cell 6 (2000) 953–959.
[45] I.S. Yuen, C. Taphouse, K.A. Halfant, R.H. Gomer, Regulation and processing of a secreted protein that mediates sensing of cell density in *Dictyostelium*, Development 113 (1991) 1375–1385.
[46] J. Calvo-Garrido, S. Carilla-Latorre, R. Escalante, Vacuole membrane protein 1, autophagy and much more, Autophagy 4 (2008) 835–837.
[47] J. Calvo-Garrido, R. Escalante, Autophagy dysfunction and ubiquitin-positive protein aggregates in *Dictyostelium* cells lacking Vmp1, Autophagy 6 (2010) 100–109.
[48] J. Calvo-Garrido, J.S. King, S. Muñoz-Braceras, R. Escalante, Vmp1 regulates PtdIns3P signaling during autophagosome formation in *Dictyostelium discoideum*, Traffic 15 (2014) 1235–1246.
[49] J. Cárcel-Trullols, A.D. Kovács, D.A. Pearce, Role of the lysosomal membrane protein, CLN3, in the regulation of cathepsin D activity, J. Cell. Biochem. 118 (2017) 3883–3890.
[50] A.L. Fabritius, J. Vesa, H.M. Minye, I. Nakano, H. Kornblum, L. Peltonen, Neuronal ceroid lipofuscinosis genes, CLN2, CLN3 and CLN5 are spatially and temporally co-expressed in a developing mouse brain, Exp. Mol. Pathol. 97 (2014) 484–491.
[51] R.J. Huber, S. Mathavarajah, Secretion and function of Cln5 during the early stages of *Dictyostelium* development, Biochim. Biophys. Acta 1865 (2018) 1437–1450.
[52] A. Lyly, C. von Schantz, C. Heine, M.L. Schmiedt, T. Sipilä, A. Jalanko, A. Kyttälä, Novel interactions of CLN5 support molecular networking between neuronal Ceroid Lipofuscinosis proteins, BMC Cell Biol. 26 (10) (2009) 83.
[53] H.M. Minye, A.L. Fabritius, J. Vesa, L. Peltonen, Data on characterizing the gene expression patterns of neuronal ceroid lipofuscinosis genes: CLN1, CLN2, CLN3, CLN5 and their association to interneuron and neurotransmission markers: Parvalbumin and Somatostatin, Data Brief. 8 (2016) 741–749.
[54] E. Scifo, A. Szwajda, J. Dębski, K. Uusi-Rauva, T. Kesti, M. Dadlez, A.C. Gingras, J. Tyynelä, M.H. Baumann, A. Jalanko, M. Lalowski, Drafting the CLN3 protein interactome in SH-SY5Y human neuroblastoma cells: a label-free quantitative proteomics approach, J. Proteome Res. 12 (2013) 2101–2115.
[55] J. Vesa, M.H. Chin, K. Oelgeschläger, J. Isosomppi, E.C. DellAngelica, A. Jalanko, L. Peltonen, Neuronal ceroid lipofuscinoses are connected at molecular level: interaction of CLN5 protein with CLN2 and CLN3, Mol. Biol. Cell 13 (2002) 2410–2420.
[56] S. Padilla-López, D.A. Pearce, *Saccharomyces cerevisiae* lacking Btn1p modulate vacuolar ATPase activity to regulate pH imbalance in the vacuole, J. Biol. Chem. 281 (2006) 10273–10280.
[57] M.T. Mazhab-Jafari, A. Rohou, C. Schmidt, S.A. Bueler, S. Benlekbir, C.V. Robinson, J.L. Rubinstein, Atomic model for the membrane-embedded VO motor of a eukaryotic V-ATPase, Nature 539 (2016) 118–122.
[58] P. Ottis, K. Koppe, B. Onisko, I. Dynin, T. Arzberger, H. Kretzschmar, J.R. Requena, C.J. Silva, J.P. Huston, C. Korth, Human and rat brain lipofuscin proteome, Proteomics 12 (2012) 2445–2454.

[59] C.H. Chan, D. Ramirez-Montealegre, D.A. Pearce, Altered arginine metabolism in the central nervous system (CNS) of the *Cln3*$^{-/-}$ mouse model of juvenile batten disease, Neuropathol. Appl. Neurobiol. 35 (2009) 189–207.
[60] P. Herrmann, C. Druckrey-Fiskaaen, E. Kouznetsova, K. Heinitz, M. Bigl, S.L. Cotman, R. Schliebs, Developmental impairments of select neurotransmitter systems in brains of Cln3(Deltaex7/8) knock-in mice, an animal model of juvenile neuronal ceroid lipofuscinosis, J. Neurosci. Res. 86 (2008) 1857–1870.
[61] N.S. Osório, A. Carvalho, A.J. Almeida, S. Padilla-Lopez, C. Leão, J. Laranjinha, P. Ludovico, D.A. Pearce, F. Rodrigues, Nitric oxide signaling is disrupted in the yeast model for batten disease, Mol. Biol. Cell 18 (2007) 2755–2767.
[62] B. Qi, X. Liu, T. Mo, S.S. Li, J. Wang, X.P. Shi, X.H. Wang, Z.X. Zhu, Y.F. Zhao, H.W. Jin, P.F. Tu, S.P. Shi, Nitric oxide inhibitory polyketides from *Penicillium chrysogenum* MT-12, an endophytic fungus isolated from Huperzia serrata, Fitoterapia 123 (2017) 35–43.
[63] D. Giustarini, R. Rossi, A. Milzani, I. Dalle-Donne, Nitrite and nitrate measurement by Griess reagent in human plasma: evaluation of interferences and standardization, Methods Enzymol. 440 (2008) 361–380.
[64] V. Sivaramakrishnan, S.J. Fountain, Evidence for extracellular ATP as a stress signal in a single-celled organism, Eukaryot. Cell 14 (2015) 775–782.
[65] M.E. Bosch, T. Kielian, Astrocytes in juvenile neuronal ceroid lipofuscinosis (CLN3) display metabolic and calcium signaling abnormalities, J. Neurochem. (2018) (in press).
[66] E.K. Shematorova, D.G. Shpakovski, A.D. Chernysheva, G.V. Shpakovski, Molecular mechanisms of the juvenile form of batten disease: important role of MAPK signaling pathways (ERK1/ERK2, JNK and p38) in pathogenesis of the malady, Biol. Direct 13 (2018) 19.
[67] M.L. Katz, K.O. Gerhardt, Storage protein in hereditary ceroid-lipofuscinosis contains S-methylated methionine, Mech. Ageing Dev. 53 (1990) 277–290.
[68] S.K. Cho, N. Gao, D.A. Pearce, M.A. Lehrman, S.L. Hofmann, Characterization of lipid-linked oligosaccharide accumulation in mouse models of batten disease, Glycobiology 15 (2005) 637–648.
[69] P.F. Daniel, D.L. Sauls, R.M. Boustany, Evidence for processing of dolichol-linked oligosaccharides in patients with neuronal ceroid-lipofuscinosis, Am. J. Med. Genet. 42 (1992) 586–592.
[70] T. Krusius, J. Viitala, J. Palo, C.P. Maury, Enrichment of high mannose-type glycans in nervous tissue glycoproteins in neuronal ceroid-lipofuscinosis, J. Neurol. Sci. 72 (1986) 1–10.
[71] R.K. Pullarkat, S.E. Zawitosky, Glycoconjugate abnormalities in the ceroid-lipofuscinoses, J. Inherit. Metab. Dis. 16 (1993) 317–322.
[72] A.E. Arrant, V.C. Onyilo, D.E. Unger, E.D. Roberson, Progranulin gene therapy improves lysosomal dysfunction and microglial pathology associated with frontotemporal dementia and neuronal ceroid lipofuscinosis, J. Neurosci. 38 (2018) 2341–2358.
[73] D.H. Paushter, H. Du, T. Feng, F. Hu, The lysosomal function of progranulin, a guardian against neurodegeneration, Acta Neuropathol. 136 (2018) 1–17.
[74] M. Stumpf, R. Müller, B. Gaßen, R. Wehrstedt, P. Fey, M.A. Karow, L. Eichinger, G. Glöckner, A.A. Noegel, A tripeptidyl peptidase 1 is a binding partner of the Golgi pH regulator (GPHR) in *Dictyostelium*, Dis. Model. Mech. 10 (2017) 897–907.
[75] G. Rot, A. Parikh, T. Curk, A. Kuspa, G. Shaulsky, B. Zupan, dictyExpress: a *Dictyostelium discoideum* gene expression database with an explorative data analysis web-based interface, BMC Bioinforma. 10 (2009) 265.
[76] A. Somogyi, A. Petcherski, B. Beckert, M. Huebecker, D.A. Priestman, A. Banning, S.L. Cotman, F.M. Platt, M.O. Ruonala, R. Tikkanen, Altered expression of ganglioside metabolizing enzymes results in GM3 ganglioside accumulation in cerebellar cells of a mouse model of juvenile neuronal ceroid lipofuscinosis, Int. J. Mol. Sci. 19 (2018) 625.
[77] M. Taniike, S. Yamanaka, R.L. Proia, C. Langaman, T. Bone-Turrentine, K. Suzuki, Neuropathology of mice with targeted disruption of Hexa gene, a model of Tay-Sachs disease, Acta Neuropathol. 89 (1995) 296–304.